

# New Heavy Quark Baryons

M. Kreps on behalf of the *BABAR*, Belle and CDF Collaborations  
*Institut für Experimentelle Kernphysik, University of Karlsruhe, Germany*

During the past year many interesting results were published in heavy quark baryon spectroscopy. In addition to several refined measurements, new states were directly observed both in the charm and the bottom sector. In this paper we review recent results on heavy quark baryons from B-factories and Tevatron experiments.

## I. INTRODUCTION

Heavy quark baryons provide, in the same way as heavy quark mesons, an interesting laboratory for studying and testing Quantum Chromodynamics (QCD), the theory of strong interactions. The heavy quark mesons provide the closest analogy to the hydrogen atom, which provided important tests of Quantum Electrodynamics. In this analogy we can consider the heavy quark meson as the "hydrogen atom" of QCD. The heavy quark baryons are the next step, where we have a state with one heavy quark and two light quarks, which are often treated together as diquark and so effectively providing the same laboratory as heavy quark mesons. The heavy quark states test regions of the QCD, where perturbation calculations cannot be used and many different approaches to solve the theory were developed. Just a few examples of them are Heavy quark effective theory, non-relativistic and relativistic potential models or lattice QCD.

From the experimental point of view, we approached a point, where several experiments collected

large data samples to study the heavy quark baryons in detail, using fully reconstructed decays. The recent results come from both the asymmetric  $e^+e^-$  B-factories with the *BABAR* and Belle experiments and the  $p\bar{p}$  collisions at Tevatron with CDF and DØ. The  $e^+e^-$  B-factories profit from huge datasets collected in a very clean environment, but their deficit is that the energy is not high enough to study b-quark baryons and are therefore limited to the charm sector. At the Tevatron on the other hand all b-quark hadrons are produced, but the price which has to be paid is a more complicated environment with huge background coming from the beam fragmentation.

In the past year many new states were observed. In addition several measurements of the properties of already known states were performed [1, 2, 3, 4]. While all of the results are certainly interesting, for space reasons we will concentrate here only on the newly observed states, which are  $\Lambda_c(2940)$ ,  $\Xi_c(2980)$  and  $\Xi_c(3077)$ ,  $\Omega_c^*$ ,  $\Sigma_b^*$  and  $\Sigma_b^*$ .

## II. $\Lambda_c$ STATES

The  $\Lambda_c$  is lowest lying baryon state in the charm sector. Together with the ground state, four other states are listed by the Particle Data Group [5]. From these states, the one with highest mass is  $\Lambda_c(2880)$  seen by the CLEO experiment [6]. As this is the first  $\Lambda_c$  state above the  $pD^0$  threshold, the *BABAR* Collaboration performed a search for the  $\Lambda_c(2880)$  in the  $p\bar{D}^0$  final state. The resulting invariant mass distribution is shown in Fig. 1 [7]. Together with the clear signal of  $\Lambda_c(2880)$  state another resonant structure is seen at a mass of  $2.94 \text{ GeV}/c^2$ . The parameters of the resonances are extracted using an unbinned maximum likelihood fit, where each of the two signals is described by a relativistic Breit-Wigner function convoluted with a Gaussian resolution function. The product of a fourth-order polynomial and two-body phase space is used for the background description. The obtained values are listed in Table I. The significance of the newly observed  $\Lambda_c(2940)^+$  is 7.5 standard deviations.

A confirmation of the newly observed state is reported by the Belle experiment in the  $\Lambda_c^+\pi^+\pi^-$  final state. The invariant mass distribution with requiring

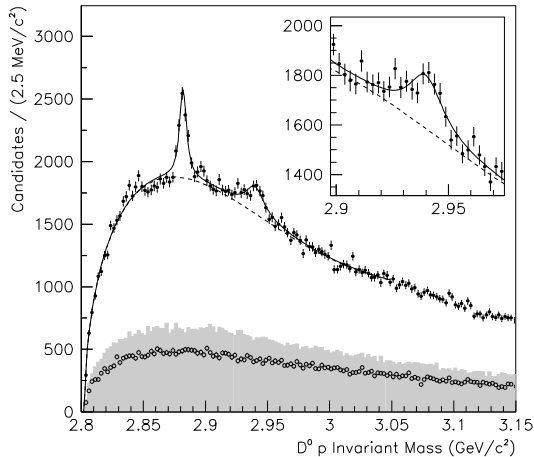


FIG. 1: Invariant mass distribution of  $pD^0$  from the *BABAR* experiment [7]. The full points show the experimental data and the open points represent wrong sign ( $p\bar{D}^0$ ) combinations. The shaded area shows data from  $D^0$  sidebands. The solid curve is the result of the fit, with the dashed line showing the background part of the fit.

TABLE I: Measured masses and widths of the new  $\Lambda_c$  and  $\Xi_c$  states.

State	BABAR		Belle	
	Mass [MeV/ $c^2$ ]	Width [MeV/ $c^2$ ]	Mass [MeV/ $c^2$ ]	Width [MeV/ $c^2$ ]
$\Lambda_c(2880)^+$	$2881.9 \pm 0.1 \pm 0.5$	$5.8 \pm 1.5 \pm 1.1$	$2881.2 \pm 0.2 \pm 0.4$	$5.5 \pm 0.7 \pm 1.1$
$\Lambda_c(2940)^+$	$2939.8 \pm 1.3 \pm 1.0$	$17.5 \pm 5.2 \pm 5.9$	$2938.0 \pm 1.3_{-4.0}^{+2.0}$	$13_{-5}^{+8}{}_{-7}^{+27}$
$\Xi_c(2980)^+$	$2967.1 \pm 1.9 \pm 1.0$	$23.6 \pm 2.8 \pm 1.3$	$2978.5 \pm 2.1 \pm 2.0$	$43.5 \pm 7.5 \pm 7.0$
$\Xi_c(2980)^0$	—	—	$2977.1 \pm 8.8 \pm 3.5$	43.5 (fixed)
$\Xi_c(3077)^+$	$3076.4 \pm 0.7 \pm 0.3$	$6.2 \pm 1.6 \pm 0.5$	$3076.7 \pm 0.9 \pm 0.5$	$6.2 \pm 1.2 \pm 0.8$
$\Xi_c(3077)^0$	—	—	$3082.8 \pm 1.8 \pm 1.5$	$5.2 \pm 3.1 \pm 1.8$

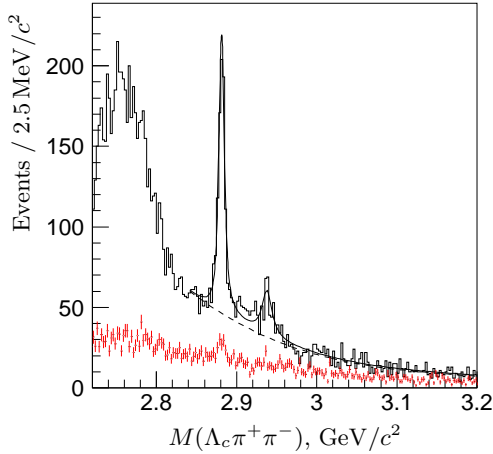


FIG. 2:  $\Lambda_c^+ \pi^+ \pi^-$  invariant mass distribution from the Belle experiment [8]. The histogram represents data with  $\Lambda_c^+ \pi^\pm$  being consistent with  $\Sigma_c(2455)$ , red dots with error bars show the scaled  $\Sigma_c(2455)$  sideband distribution. The full and dashed lines represent the result of the fit and the background part of the fit.

the  $\Lambda_c^+ \pi^\pm$  invariant mass to be consistent with the  $\Sigma_c(2455)$  is shown in Fig. 2 [8]. Three signals corresponding to  $\Lambda_c(2765)^+$ ,  $\Lambda_c(2880)^+$  and  $\Lambda_c(2940)^+$  are clearly visible in the distribution. Using a binned maximum likelihood fit with two signals and a third-order polynomial background the masses and widths of the  $\Lambda_c(2880)^+$  and  $\Lambda_c(2940)^+$  states are extracted. The resulting parameters are listed in Table I and are consistent with those measured by the *BABAR* experiment. The significance of the  $\Lambda_c(2940)^+$  state is found to be 6.2 standard deviations.

To gain more information on the two  $\Lambda_c$  states, both experiments perform additional studies. A first question to which the experiments try to find an answer is whether the  $\Lambda_c(2940)^+$  and  $\Lambda_c(2880)^+$  are really  $\Lambda_c$  states and not  $\Sigma_c$  states. In the case when the observed states are  $\Sigma_c$  states, one also expects signals in the  $pD^+$  invariant mass distribution. *BABAR* performs this study, the result of which is shown in Fig. 3. None of the two signals are visible from which one

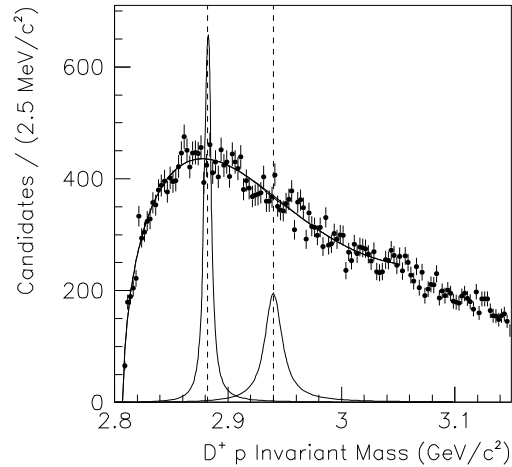


FIG. 3:  $pD^+$  invariant mass distribution from the *BABAR* experiment [7]. The points with error bars show data, the curve through the points is the result of the fit. The two peaks show the expected signal if the two states at 2880 and 2940 MeV/ $c^2$  would be produced with the same rate as in the  $pD^0$  final state.

concludes, that the observed states are  $\Lambda_c$  states. For illustration, the two peaks in Fig. 3 show expected signals if the states would be  $\Sigma_c$  states produced with the same rate as in the  $pD^0$  channel.

The Belle experiment uses a different approach and uses a high statistics signal for the  $\Lambda_c(2880)^+$  state to study the resonant substructure of its decay to  $\Lambda_c^+ \pi^+ \pi^-$ . Also an analysis of the angular distributions is done to constrain the  $\Lambda_c(2880)^+$  quantum numbers. To gain more statistics, these studies are done with looser cuts compared to the ones used for the invariant mass distribution of Fig. 2. To obtain the sub-resonant structure of the decay, fits of  $\Lambda_c^+ \pi^+ \pi^-$  invariant mass distributions in slices of the invariant mass  $M(\Lambda_c^+ \pi^\pm)$  are done. The obtained distributions of  $\Lambda_c(2880)^+$  events is shown in Fig. 5. A clear signal for the  $\Sigma_c(2455)$  is visible together with a structure at the mass of the  $\Sigma_c(2520)$  state. The significance of the  $\Sigma_c(2520)$  signal is esti-

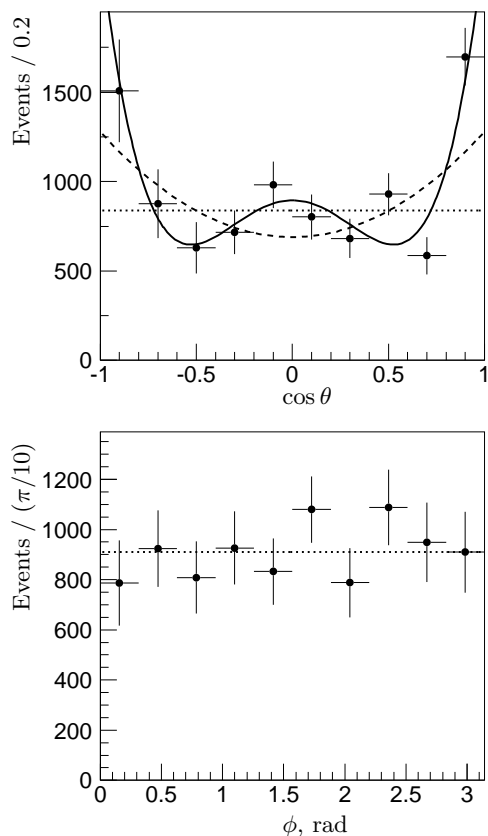


FIG. 4: The yield of  $\Lambda_c(2880)^+ \rightarrow \Sigma_c \pi$  decays as a function of  $\cos \theta$  and  $\phi$ . The lines show the fit for  $J = 1/2$  (dotted),  $J = 3/2$  (dashed) and  $J = 5/2$  (full) hypothesis.

mated to be 3.7 standard deviations. The resulting ratios of partial widths are  $\frac{\Gamma(\Sigma_c(2455)\pi^\pm)}{\Gamma(\Lambda_c^+\pi^+\pi^-)} = 0.404 \pm 0.021 \pm 0.014$ ,  $\frac{\Gamma(\Sigma_c(2520)\pi^\pm)}{\Gamma(\Lambda_c^+\pi^+\pi^-)} = 0.091 \pm 0.025 \pm 0.010$  and  $\frac{\Gamma(\Sigma_c(2520)\pi^\pm)}{\Gamma(\Sigma_c(2455)\pi^\pm)} = 0.225 \pm 0.062 \pm 0.025$ . The angular analysis uses the helicity angle  $\theta$  and the angle  $\phi$  between the  $e^+e^- \rightarrow \Lambda_c(2880)^+ X$  reaction plane and a plane defined by the pion momentum and the  $\Lambda_c(2880)^+$  boost direction in the  $\Lambda_c(2880)^+$  rest frame. The measured angular distributions are shown in Fig. 4. The distribution of  $\phi$  is found to be uniform, which is consistent with a  $J = 1/2$  hypothesis. The  $J = 3/2$  and  $J = 5/2$  hypotheses, which are considered as well, can have a uniform  $\phi$  distribution but doesn't have to. In the description of the  $\cos \theta$  distribution for all three hypotheses only terms consistent with a flat  $\phi$  distributions are used. By a  $\chi^2$  comparison it is concluded, that the most probable assignment is  $J = 5/2$  and that the two lower spins can be excluded by 5.5 or 4.8 standard deviations. Having determined the spin of the state, we can return to the measurement of  $R = \frac{\Gamma(\Sigma_c(2520)\pi^\pm)}{\Gamma(\Sigma_c(2455)\pi^\pm)}$ . Heavy quark symmetry predicts  $R = 1.4$  for a  $5/2^-$  state and

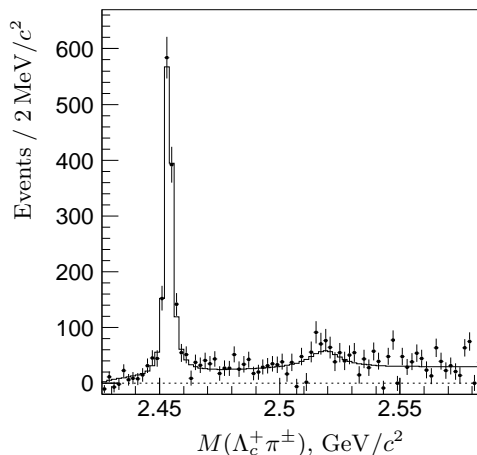


FIG. 5: The  $\Lambda_c(2880)^+$  yield as a function of the invariant mass of  $\Lambda_c^+ \pi^\pm$ . The histogram shows the result of the fit.

$R = 0.23 - 0.36$  for a  $5/2^+$  state. Comparing the prediction to the measured value, Belle concludes that the  $\Lambda_c(2880)^+$  state has quantum numbers  $J^P = 5/2^+$ .

Here we would like to point out, that a state at 2765 MeV/ $c^2$  is listed by the Particle Data Group [5], but its nature is unknown. It would certainly be important to perform more studies of this state to find out, whether it is a  $\Lambda_c$  or  $\Sigma_c$  excitation and to perform an angular analysis to constrain the quantum numbers of this state. Certainly both experiments at the B-factories should have enough data to perform such an analysis.

### III. $\Xi_c$ STATES

Another particle for which new states are observed during the last year is the  $\Xi_c$ . One motivation is the observation of the double charmed baryon  $\Xi_{cc}$  in the  $\Lambda_c^+ K^- \pi^+$  final state reported by the SELEX collaboration [9]. The other is that charmed strange baryons should decay to this final state if they are above threshold, but none of the states seen up to now have high enough mass. In this situation the Belle collaboration performs a search for the new baryons in the  $\Lambda_c^+ K^- \pi^+$  and  $\Lambda_c^+ K_s^0 \pi^+$  final states. The invariant mass distributions in both decay modes are shown in Fig. 6 [10]. Two clear peaks are visible in the  $\Lambda_c^+ K^- \pi^+$  final state and one in the  $\Lambda_c^+ K_s^0 \pi^+$  final state. From an maximum likelihood fit the masses, widths, numbers of events and significances are extracted. The fit returns  $405.3 \pm 50.7$  signal events for the  $\Xi_c(2980)^+$  state and  $326.0 \pm 39.6$  signal events for the  $\Xi_c(3077)^+$ . The significances of the two states are 5 and 9 standard deviations. In the case of the neutral combination the fit results in  $67.1 \pm 19.9$  events for the  $\Xi_c(3077)^0$  and  $42.3 \pm 23.8$  events for the  $\Xi_c(2980)^0$ .

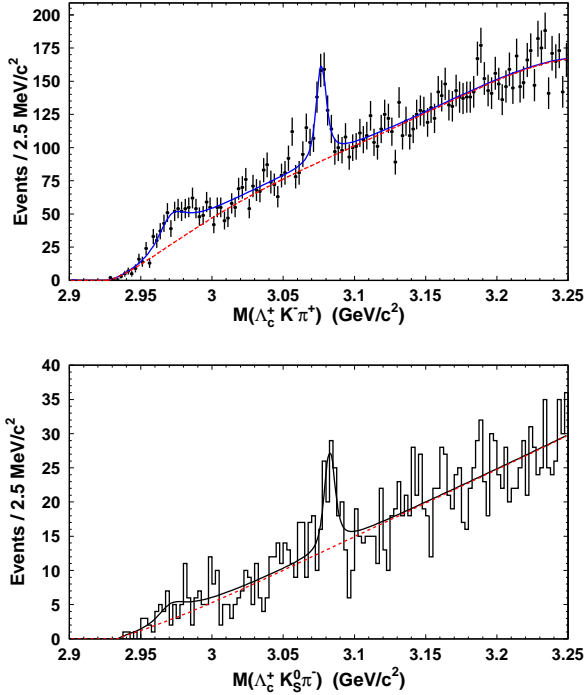


FIG. 6: Distribution of the invariant mass distribution of  $\Lambda_c^+ K^- \pi^+$  combinations (top) and  $\Lambda_c^+ K_s^0 \pi^+$  combinations (bottom) [10]. The points represent data, the full (blue) line corresponds to the fit result and the dashed (red) line to the background part of the fit.

Due to the low statistics the width of the  $\Xi_c(2980)^0$  state was fixed to be the same as for the charged state. The significance of the  $\Xi_c(3077)^0$  is 4 standard deviations, while the statistical significance of the  $\Xi_c(2980)^0$  state is 1.5 standard deviations. The obtained masses and widths are listed in Table I. The interpretation of the newly observed states as  $\Xi_c$ 's can unambiguously be derived from the quark content of the particles in the final state, which gives the quark content of a  $\Xi_c$  baryon.

The observation of the  $\Xi_c(2980)^+$  and  $\Xi_c(3077)^+$  states is confirmed by the *BABAR* experiment using the  $\Lambda_c^+ K^- \pi^+$  decay mode [11]. The invariant mass difference distribution is shown in Fig. 7. Structures at the masses of the two new  $\Xi_c$  states seen by Belle are also visible here. The *BABAR* collaboration doesn't exploit neutral charge combinations, but rather goes further and studies the resonance substructure of the decays of the  $\Xi_c(2980)^+$  and  $\Xi_c(3077)^+$  states. In the first step, the dalitz plots of  $M(\pi^+ K^-)$  versus  $M(\Lambda_c^+ \pi^+)$  in the four shaded regions in Fig. 7 are examined. In the dalitz distributions for which we kindly refer reader to work [11], a clear structure corresponding to the  $\Sigma_c(2455)^{++}$  and the  $\Sigma_c(2520)^{++}$  are visible in both signal and sideband regions. In the final extended maximum likelihood fit

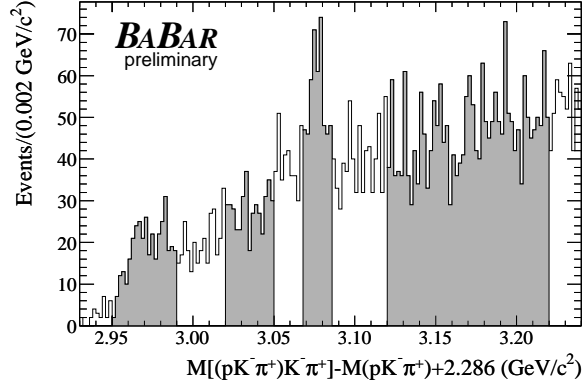


FIG. 7: Distribution of the invariant mass difference of  $\Lambda_c^+ K^- \pi^+$  from the *BABAR* experiment [11]. The shaded regions were used for dalitz plots, which can be found in the original work [11].

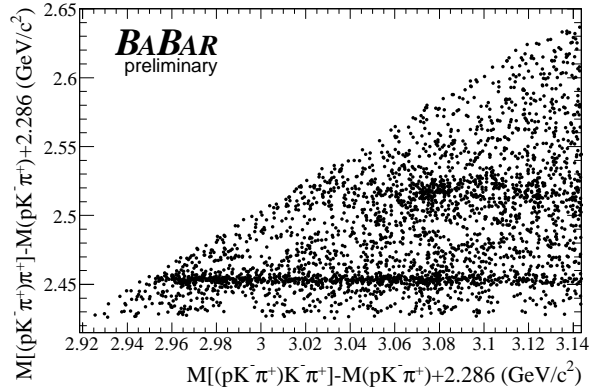


FIG. 8: A two-dimensional distribution of  $M(\Sigma_c)$  versus  $M(\Xi_c)$  used in the fit to extract  $\Xi_c$  states parameters. The two horizontal bands correspond to the  $\Sigma_c(2455)^{++}$  and  $\Sigma_c(2520)^{++}$  states.

of  $\Lambda_c^+ K^- \pi^+$  and  $\Lambda_c^+ \pi^+$  masses the amount of decays through  $\Sigma_c(2455)^{++}$ ,  $\Sigma_c(2520)^{++}$  and non-resonant  $\Lambda_c^+ K^- \pi^+$  is extracted. The two dimensional distribution of  $M(\Lambda_c^+ \pi^+)$  versus  $M(\Lambda_c^+ K^- \pi^+)$  used in the fit is shown in Fig. 8. Figure 9 shows fit projections onto  $M(\Lambda_c^+ \pi^+)$  and  $M(\Lambda_c^+ K^- \pi^+)$ . The fit returns  $284 \pm 45 \pm 46$  signal events for the  $\Xi_c(2980)^+$  with a significance of 7 standard deviations and  $204 \pm 35 \pm 12$  signal events with a significance of 8.6 standard deviations for the  $\Xi_c(3077)^+$ . The extracted masses and widths are listed in Table I. Results for the  $\Xi_c(3077)^+$  agree well between Belle and *BABAR*, while for the  $\Xi_c(2980)^+$  there is a slight discrepancy between the two experiments. The yields and significances of different resonant and non-resonant decays are listed in Table II. Except of the non-resonant component of  $\Xi_c(3077)^+$  decay, all others are in the range from 4 to

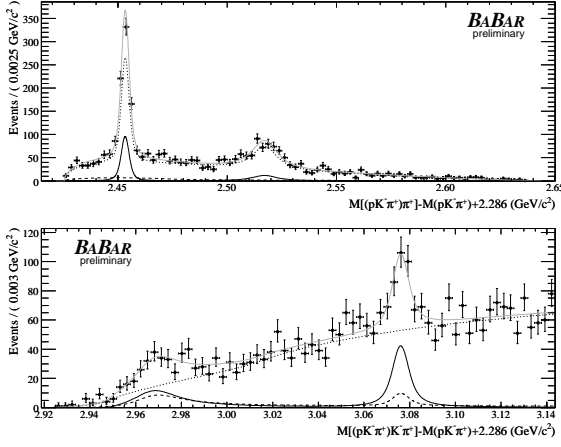


FIG. 9: Projections of the fit onto the mass variables  $M(\Lambda_c^+ \pi^+)$  (top) and  $M(\Lambda_c^+ K^- \pi^+)$  (bottom). The points represent data and the solid grey curves the full fit. The signal component with the  $\Sigma_c^{++}$  intermediate states are shown by the solid dark curve and the non-resonant part of the decay by the dashed curve. The fitted background is shown by the dotted curve.

TABLE II: Yields and significances for the separate resonant and non-resonant decays of the  $\Xi_c(2980)^+$  and  $\Xi_c(3077)^+$  states [11].

	Events	Significance
$\Xi_c(2980)^+ \rightarrow \Sigma_c(2455)^{++} K^-$	$132 \pm 31 \pm 5$	$4.9 \sigma$
$\Xi_c(2980)^+ \rightarrow \Lambda_c^+ K^- \pi^+$	$152 \pm 37 \pm 45$	$4.1 \sigma$
$\Xi_c(3077)^+ \rightarrow \Sigma_c(2455)^{++} K^-$	$87 \pm 20 \pm 4$	$5.8 \sigma$
$\Xi_c(3077)^+ \rightarrow \Sigma_c(2520)^{++} K^-$	$82 \pm 23 \pm 6$	$4.6 \sigma$
$\Xi_c(3077)^+ \rightarrow \Lambda_c^+ K^- \pi^+$	$35 \pm 24 \pm 16$	$1.4 \sigma$

6 standard deviations. For both new  $\Xi_c$  states the decays through  $\Sigma_c(2455)$  and  $\Sigma_c(2520)$  resonances forms a large part of the observed decays.

For the future, both states can benefit from further studies. On the one hand, a confirmation on 5 standard deviations level for the neutral states should be done. The other direction clearly is to establish spin and parity of the new states.

#### IV. OBSERVATION OF THE $\Omega_c^*$ STATE

In the charm sector, all singly charmed states with zero orbital momentum have been discovered [5] except the  $\Omega_c^*$ . The theoretical expectations for the mass difference between the  $\Omega_c^*$  and the  $\Omega_c$  are in the range from 50 to 104 MeV/c<sup>2</sup> [13, 14, 15, 16, 17, 18, 19, 20, 21, 22]. In the work of the BABAR experiment [12] a search for the  $\Omega_c^*$  through its radiative decay is

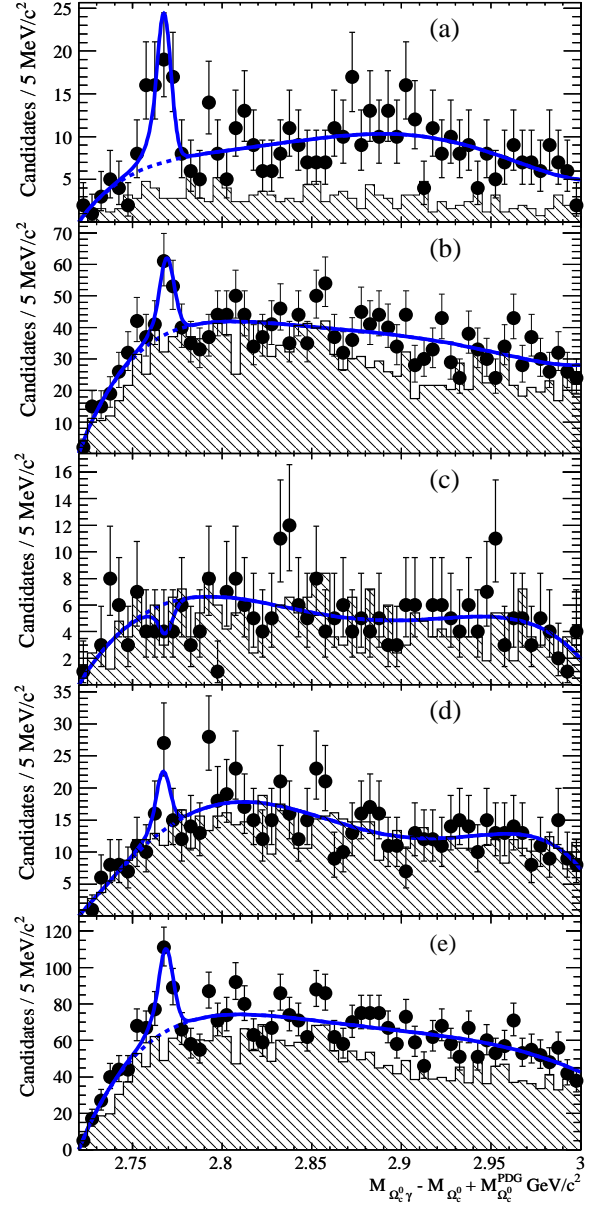


FIG. 10: The invariant mass difference distributions of  $\Omega_c^* \rightarrow \Omega_c \gamma$  candidates, with the  $\Omega_c$  reconstructed in (a)  $\Omega^- \pi^+$ , (b)  $\Omega^- \pi^+ \pi^0$ , (c)  $\Omega^- \pi^+ \pi^- \pi^+$ , (d)  $\Xi^- K^- \pi^+ \pi^+$  decay mode and (e) combining all decay modes together. The points with error bars represent data and the dashed line distribution from the  $\Omega_c$  sidebands. The full line represents the result of the fit and the dashed line the combinatorial background.

performed. The  $\Omega_c$  is reconstructed in the following decay modes

$$\begin{aligned} \Omega_c^0 &\rightarrow \Omega^- \pi^+ & \Omega_c^0 &\rightarrow \Omega^- \pi^+ \pi^0 \\ \Omega_c^0 &\rightarrow \Omega^- \pi^+ \pi^- \pi^+ & \Omega_c^0 &\rightarrow \Xi^- K^- \pi^+ \pi^+ \end{aligned}$$

with  $\Omega^- \rightarrow \Lambda K^-$  and  $\Xi^- \rightarrow \Lambda \pi^-$ . In total around 300  $\Omega_c$  signal events are reconstructed in all four de-

TABLE III: The mass difference  $\Delta M = M(\Omega_c^*) - M(\Omega_c)$ , the fitted signal yield  $Y$  (events) and the  $\Omega_c^*$  signal significance using different  $\Omega_c$  decay modes.

Decay mode	$\Delta M$ (MeV/ $c^2$ )	$Y$ (Events)	$S$ ( $\sigma$ )
$\Omega_c^0 \rightarrow \Omega^- \pi^+$	$69.9 \pm 1.4 \pm 1.0$	$39_{-9}^{+10} \pm 6$	4.2
$\Omega_c^0 \rightarrow \Omega^- \pi^+ \pi^0$	$71.8 \pm 1.3 \pm 1.1$	$55_{-15}^{+16} \pm 6$	3.4
$\Omega_c^0 \rightarrow \Omega^- \pi^+ \pi^- \pi^+$	69.9 (fixed)	$-5 \pm 5 \pm 1$	-
$\Omega_c^0 \rightarrow \Xi^- K^- \pi^+ \pi^+$	$69.4_{-2.0}^{+1.9} \pm 1.0$	$20 \pm 9 \pm 3$	2.0
Combined	$70.8 \pm 1.0 \pm 1.1$	$105 \pm 21 \pm 6$	5.2

cay modes. The  $\Omega_c$  candidates are then combined with a photon to form  $\Omega_c^*$  candidates. The invariant mass difference distributions in the four different  $\Omega_c$  decay modes are shown in Fig. 10. In the two decay modes with the highest  $\Omega_c$  signal, a clear peak in the  $\Omega_c \gamma$  invariant mass difference distribution is visible, see Fig. 10(a) and 10(b). In the other two modes one mode has an indication for a signal, while the other one has not. The maximum likelihood fit in each  $\Omega_c$  decay mode yields consistent mass differences  $\Delta M = M(\Omega_c^*) - M(\Omega_c)$  and widths across the  $\Omega_c$  decay modes (see Table III). As the separate decay modes are consistent, we can combine them together and perform a single maximum likelihood fit. The result of the fit is shown in Fig. 10(e) and yields  $\Delta M = 70.9 \pm 1.0 \pm 1.1 \text{ MeV}/c^2$  with  $105 \pm 21 \pm 6$  signal events. The significance of the signal including systematic uncertainty is 5.2 standard deviations.

## V. OBSERVATION OF CHARGED $\Sigma_b$ AND $\Sigma_b^*$

Up to recently, the  $\Lambda_b$  was the only directly observed  $b$ -baryon. With increasing data samples collected at the Tevatron accelerator, the searches for other  $b$ -baryons starts to be feasible. The first of such searches was performed by the CDF experiment, which searched for the  $\Sigma_b$  baryon and its spin excited partner  $\Sigma_b^*$  [23]. A general theoretical expectations [13, 22, 24, 25, 26, 27, 28, 29, 30, 31, 32, 33, 34, 35, 36, 37, 38] are the mass difference  $M(\Sigma_b) - M(\Lambda_b) - M(\pi) = 40 - 70 \text{ MeV}/c^2$  with  $M(\Sigma_b^*) - M(\Sigma_b) = 10 - 40 \text{ MeV}/c^2$ . A small difference on the level of  $5 \text{ MeV}/c^2$  is expected between the masses of  $\Sigma_b^+$  and  $\Sigma_b^-$ . Both the  $\Sigma_b$  and the  $\Sigma_b^*$  are expected to be narrow with a natural width of around 8 and  $15 \text{ MeV}/c^2$  with  $\Lambda_b \pi$  being the dominant decay mode.

The CDF search is based on  $1 \text{ fb}^{-1}$  of data using fully reconstructed  $\Lambda_b$  baryons. The  $\Lambda_b$  is reconstructed in the  $\Lambda_c \pi$  decay mode with  $\Lambda_c \rightarrow p K^- \pi^+$ . In total around 3000  $\Lambda_b$  signal events are reconstructed. In the sample used for the  $\Sigma_b$  search 86 % of events are  $\Lambda_b$  baryons. The search is performed

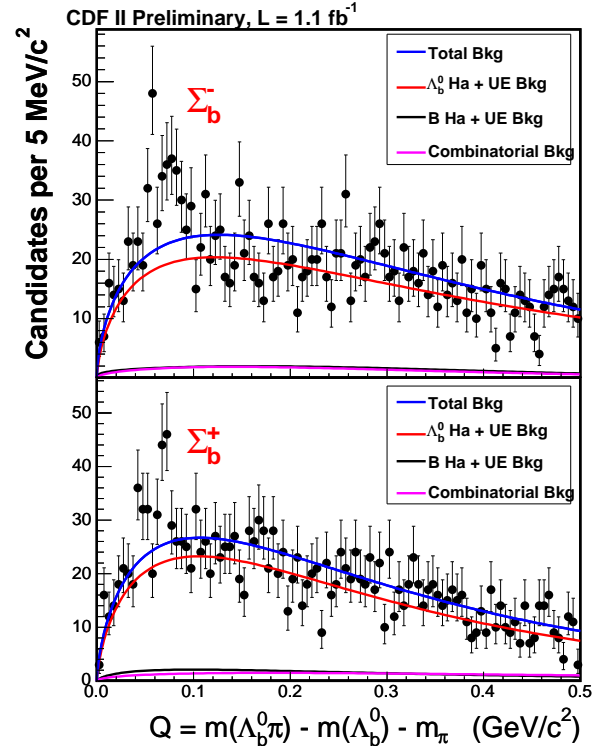


FIG. 11: The invariant mass difference distribution of the  $\Sigma_b^\pm$  candidates. The points with error bars represent data, the blue line represents the predicted background, while the other three lines show three separate background contributions.

for the charged  $\Sigma_b$ 's only, as the neutral one decays by emission of  $\pi^0$ , which is extremely difficult to detect at the CDF experiment.

The selected  $\Lambda_b$  candidates are then combined with charged pions to form  $\Sigma_b$  candidates. After fixing the selection of candidates, the background is estimated while keeping the signal region blinded. The background consists of three basic components, which are combinatorial background,  $\Lambda_b$  hadronization and hadronization of mis-reconstructed  $B$  mesons. Relative fractions of these components are taken from the

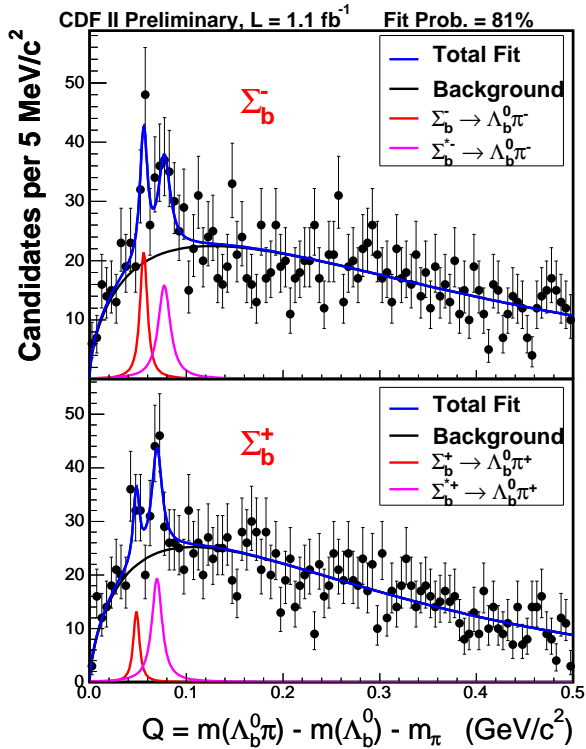


FIG. 12: Projection of the fit result of the  $\Sigma_b$  invariant mass difference distribution. The points with error bars represent data. The blue line corresponds to the result of the fit, the background is shown by the black line while the signals are represented by the red and magenta curves.

fit of the  $\Lambda_b$  invariant mass distribution. The shape of the combinatorial background is determined using the upper sideband of the  $\Lambda_b$  invariant mass distribution. For the hadronization of mis-reconstructed  $B$  mesons the fully reconstructed  $B^0 \rightarrow D^-\pi^+$  in the data are used. The shape of the largest component,  $\Lambda_b$  hadronization, is determined using a PYTHIA Monte Carlo sample. The unblinded mass difference distributions with the predicted background are shown in Fig. 11. For the both charges a clear excess above the predicted background is visible in the signal region ( $Q \in [30, 100] \text{ MeV}/c^2$ ). The number of background events predicted in the signal region is 268 for  $\Sigma_b^-$  and 298 for  $\Sigma_b^+$ . In the data we observe 416 events for negatively charged candidates and 406 for positively charged ones.

To extract the signal yields and positions of the peaks, an unbinned maximum likelihood fit is performed. The data are described by a previously determined background shape together with Breit-Wigner functions convoluted with a resolution function for each peak. Due to the low statistics,  $M(\Sigma_b^{*+}) - M(\Sigma_b^+)$  is constrained to be the same as  $M(\Sigma_b^{*-}) - M(\Sigma_b^-)$ . The values obtained in the fit are summa-

TABLE IV: Result of the fit to the  $\Sigma_b$  invariant mass difference distribution.

Parameter	Value
$Q(\Sigma_b^+)$ (MeV/ $c^2$ )	$48.4^{+2.0}_{-2.3} \pm 0.1$
$Q(\Sigma_b^-)$ (MeV/ $c^2$ )	$55.9^{+1.0}_{-1.0} \pm 0.1$
$M(\Sigma_b^*) - M(\Sigma_b)$ (MeV/ $c^2$ )	$21.3^{+2.0+0.4}_{-1.9-0.2}$
$\Sigma_b^+$ events	$29^{+12.4+5.0}_{-11.6-3.4}$
$\Sigma_b^-$ events	$60^{+14.8+8.5}_{-13.8-4.0}$
$\Sigma_b^{*+}$ events	$74^{+17.2+10.3}_{-16.3-5.7}$
$\Sigma_b^{*-}$ events	$74^{+18.2+15.6}_{-17.4-5.0}$

rized in Table IV and the fit projection is shown in Fig. 12.

To estimate the significance of the observed signal, the fit is repeated with alternative hypothesis and difference in the likelihoods is used. Three different alternative hypotheses were examined, namely the null hypothesis, using only two peaks instead of four and leaving each single peak separately out of the fit. As a result we conclude, that the null hypothesis can be excluded by more than 5 standard deviations. The fit also clearly prefers four peaks against two and except of the  $\Sigma_b^+$  peak, each peak has a significance above three standard deviations.

## VI. CONCLUSIONS

The heavy quark baryons provide an interesting laboratory for testing various approaches to the non-perturbative regime of Quantum Chromodynamics. In the past year several new states were discovered in the charm sector by the Belle and BABAR experiments and the charged  $\Sigma_b$  and  $\Sigma_b^*$  baryons in the bottom sector by the CDF experiment. The important point is that experimentalists don't stop at the observation and the mass and width measurements of the new states, but try to go beyond to learn more. Certainly the angular analyzes to determine the quantum numbers of the new states together with the detailed studies of the production and decays is important to learn more about heavy quark baryons in general.

We conclude, that the last year was very productive in experimental studies of the heavy quark baryons with several important observations of new states. Probably the two most important ones are the observation of the  $\Omega_c^*$  and the charged  $\Sigma_b^{(*)}$  baryons. With still increasing datasets and current encouraging results we are convinced that more new results can be expected in the upcoming year.

### Acknowledgments

The author would like to thank all his colleagues from the *BABAR*, Belle and CDF experiments, who

contributed to the preparation of this talk and proceedings by checking the material and giving useful comments.

- 
- [1] K. Abe *et al.* [Belle Collaboration], arXiv:hep-ex/0608012.
  - [2] B. Aubert *et al.* [BABAR Collaboration], arXiv:hep-ex/0703030.
  - [3] B. Aubert *et al.* [BABAR Collaboration], Phys. Rev. D **74** (2006) 011103.
  - [4] B. Aubert *et al.* [BABAR Collaboration], arXiv:hep-ex/0607086.
  - [5] W. M. Yao *et al.* [Particle Data Group], J. Phys. G **33** (2006) 1.
  - [6] M. Artuso *et al.* [CLEO Collaboration], Phys. Rev. Lett. **86** (2001) 4479.
  - [7] B. Aubert *et al.* [BABAR Collaboration], Phys. Rev. Lett. **98** (2007) 012001.
  - [8] K. Abe *et al.* [Belle Collaboration], arXiv:hep-ex/0608043.
  - [9] M. Mattson *et al.* [SELEX Collaboration], Phys. Rev. Lett. **89** (2002) 112001.
  - [10] R. Chistov *et al.* [BELLE Collaboration], Phys. Rev. Lett. **97** (2006) 162001.
  - [11] B. Aubert *et al.* [BABAR Collaboration], arXiv:hep-ex/0607042.
  - [12] B. Aubert *et al.* [BABAR Collaboration], Phys. Rev. Lett. **97** (2006) 232001. (2006).
  - [13] N. Mathur, R. Lewis and R. M. Woloshyn, Phys. Rev. D **66**, 014502 (2002).
  - [14] R. M. Woloshyn, Nucl. Phys. Proc. Suppl. **93**, 38 (2001).
  - [15] L. Burakovsky, T. Goldman and L. P. Horwitz, Phys. Rev. D **56**, 7124 (1997).
  - [16] M. J. Savage, Phys. Lett. B **359**, 189 (1995).
  - [17] J. L. Rosner, Phys. Rev. D **52**, 6461 (1995).
  - [18] R. Roncaglia, D. B. Lichtenberg and E. Predazzi, Phys. Rev. D **52**, 1722 (1995).
  - [19] D. B. Lichtenberg, R. Roncaglia and E. Predazzi, Phys. Rev. D **53**, 6678 (1996).
  - [20] A. Zalewska and K. Zalewski, arXiv:hep-ph/9608240.
  - [21] L. Y. Glozman and D. O. Riska, Nucl. Phys. A **603**, 326 (1996) [Erratum-ibid. A **620**, 510 (1997)].
  - [22] E. Jenkins, Phys. Rev. D **54**, 4515 (1996).
  - [23] A. Abulencia *et al.* (CDF Collaboration), CDF Public Note 8651.
  - [24] D. P. Stanley and D. Robson, Phys. Rev. Lett. **45** (1980) 235.
  - [25] D. P. Stanley and D. Robson, Phys. Rev. D **21** (1980) 3180.
  - [26] D. Izatt, C. DeTar and M. Stephenson, Nucl. Phys. B **199** (1982) 269.
  - [27] D. B. Lichtenberg, R. Roncaglia, J. G. Wills and E. Predazzi, Z. Phys. C **47** (1990) 83.
  - [28] A. Martin and J. M. Richard, Phys. Lett. B **185** (1987) 426.
  - [29] J. M. Richard and P. Taxil, Phys. Lett. B **128** (1983) 453.
  - [30] J. L. Basdevant and S. Boukraa, Z. Phys. C **30** (1986) 103.
  - [31] K. C. Bowler *et al.* [UKQCD Collaboration], Phys. Rev. D **54** (1996) 3619.
  - [32] E. Jenkins, Phys. Rev. D **55** (1997) 10.
  - [33] C. Albertus, J. E. Amaro, E. Hernandez and J. Nieves, Nucl. Phys. A **740** (2004) 333.
  - [34] D. Ebert, R. N. Faustov and V. O. Galkin, Phys. Rev. D **72** (2005) 034026.
  - [35] W. Y. P. Hwang and D. B. Lichtenberg, Phys. Rev. D **35** (1987) 3526.
  - [36] S. Capstick, Phys. Rev. D **36** (1987) 2800.
  - [37] W. Kwong, J. L. Rosner and C. Quigg, Ann. Rev. Nucl. Part. Sci. **37** (1987) 325.
  - [38] M. Karliner and H. J. Lipkin, arXiv:hep-ph/0307243.